Catal Lett (2011) 141:1643–1650
DOI 10.1007/s10562-011-0685-0

Role of CeO_2 in Rh/α-Al_2O_3 Catalysts for CO_2 Reforming of Methane

Marco Ocsachoque · Jose Bengoa · Delia Gazzoli · María Gloria González

Received: 3 November 2010 / Accepted: 10 August 2011 / Published online: 7 September 2011

Abstract The Rh/α-Al_2O_3 catalyst was modified by CeO_2 in order to improve the thermal stability and the carbon deposition resistance during the CO_2 reforming of methane The carbon formation was determined by TPO, TEM and Raman spectroscopy. Characterization results showed that the incorporation of Ce in the support inhibits the carbon deposition, increasing the useful life and the stability of the Rh base catalysts.

Keywords Rh catalyst · Dry reforming of methane · Carbon deactivation · CeO_2-αAl_2O_3 · Heterogeneous catalysis

1 Introduction

During the last years the reforming of methane with CO_2 has received great attention, from the perspective of global warming and alternative energy sources [1, 2]. This process is of great interest due to its potentially friendly effect on the environment by transforming two greenhouses in products of industrial interest. Another advantage is the possible location of synthesis gas plants in areas where water is not available with the quality and quantities required for steam reforming. The dry reforming of methane (DRM) is an important route in the use of biomass as renewable energy source for biogas conversion (60% CH_4 and 40% CO_2) to synthesis gas. Thus, the biogas would be converted to a commodity with added value and would contribute to reduce CO_2 emissions to the atmosphere.

The natural gas dry reforming process is limited in industrial applications by its thermodynamic potential for coke formation which produces a low stability in time. Just to this problem, there is increasing interest to develop catalysts that minimize the deactivation and increase their useful life. Supported noble metals have promising high catalytic performances and low sensitivities to carbon deposition during the reforming process. In the literature it is found that the supported Pt [3–6], Rh [7, 8] and Pd [9] catalysts are active and stable for this reaction. However, it is important, by the low availability and high cost, to develop active catalysts with very low noble metal content. The Rh catalysts show high activity for CO_2 reforming of methane and increase the resistance to carbon formation by oxidation of carbonaceous species adsorbed during the methane dissociation on the metal [10–12]. Another possibility to increase the durability and stability of DRM catalysts is the modification of support and the active phase by means of the addition of alkali and/or rare earth oxides [13–16]. These changes in the formulation of catalysts lead to improve stability because they inhibit the formation of carbon and metal sintering [17]. It has been reported that the addition of ceria improves the behavior of alumina based catalysts [18] as an effective promoter. CeO_2 is considered a material with a large capacity to store oxygen, great capacity to undergo cycles of oxidation–reduction that facilitate the mobility of active species on the catalyst surface by means of spill over mechanism, by this way, it provides oxygen to the metal during the reaction and

M. Ocsachoque · M. G. González (✉)
Department of Chemistry, Universidad Nacional de La Plata, Buenos Aires, Argentina
e-mail: mgg@quimica.unlp.edu.ar

J. Bengoa
Comisión de Investigaciones de la Pcia Bs As, Buenos Aires, Argentina

D. Gazzoli
Universita di Roma "La Sapienza", Rome, Italy

suppresses carbon deposition. The contribution of ceria is very important in steam reforming, water gas shift and NO reduction reactions over metal catalysts. It has been reported [19, 20] that Ni supported on CeO_2 is about 20 times more active than Ni supported on SiO_2 in steam reforming. A number of CeO_2 based systems have been examined for their catalytic properties in industrial catalysts [21]. Kugai et al. [22] studied how the CeO_2 affects the performance of Ni-Rh/CeO_2 catalyst in the oxidative steam reforming of ethanol for fuel cell applications. Ceria doping improved methane conversion and syngas selectivity for Rh/ZrO_2 during partial oxidation of methane. The effect is related to a significantly higher Rh dispersion on the CeO_2–ZrO_2 support [23]. There is great interest in using ceria in the reforming of methane at the anodes of solid oxide fuel cells (SOFC), where potential deactivation by carbon deposition is very important [24, 25].

The aim of this work is to study the role of CeO_2 as a promoter of Rh (0.5%)/Al_2O_3 catalyst, on the activity, stability and carbon deposition during the methane reforming with CO_2.

2 Experimental

2.1 Preparation of Catalysts

The supports used were CeO_2–Al_2O_3 (3 or 5 wt% CeO_2 impregnated on α-Al_2O_3, S_{BET}: 5 m^2 g^{-1}, Vp: 0.01 cm^3 g^{-1}) previously dried at 100 °C and calcined at 500 °C for 1 h in air. The catalysts containing 0.5 wt% Rh were prepared by incipient wetness impregnation using aqueous solution of rhodium chloride. The impregnated supports were dried at 100 °C followed by calcination at 350 or 500 °C for 1 h. Under this methodology, the following series of catalysts were obtained: Rh/Ce(x)Al (T) and Rh/Al(T), where x and T correspond to the CeO_2 wt% content and calcination temperature, respectively. Previously to the catalytic test, the samples were reduced in situ with pure hydrogen at 650 °C for 1 h.

2.2 Catalyst Characterization

Catalysts were characterized by N_2 gas adsorption (BET), H_2 chemisorption, X-ray diffraction (XRD), temperature programmed reduction (TPR), and thermogravimetric analysis (TGA) in order to analyze the physicochemical properties and their effect on the catalytic properties, with special emphasis in deactivation problems.

The BET surface area and pore volume distribution were measured by N_2 adsorption at −196 °C in an Accusorb 2100E Micromeritics analyzer. Samples were outgassed at 100 °C for 12 h before adsorption.

The Rh dispersion (D) and metallic area (A_{Rh}) were determined by static equilibrium H_2 chemisorption method, assuming a stoichiometry $Rh/H_2 = 2$ and the area occupied by each Rh atom was 7.5 A^2. All samples previously reduced were again exposed to a in situ reduction in hydrogen flow of 60 cm^3 min^{-1} from RT up to 250 °C and maintaining for 1 h. Then the samples were outgassed in high-vacuum for 3 h at 110 °C and 1 h at 250 °C and after that, they were cooled down to 40 °C. Adsorption isotherms were measured at room temperature in the range 134–565 mbar. The mean particle size (dp) of catalysts was calculated by $dp = 543/A_{Rh}$, assuming that the particle is spherical and wholly exposed to adsorption.

The identification of the species present in the catalysts were determined by XRD using Philips PW 1740 equipment with CuKα radiation, under 30 mA current and 40 kV voltages and a continuous scan angle 2 (was selected from 5 to 70°).

Reducibility of the samples was determined in a TPR conventional equipment using 0.1 g of catalyst and 10% (v/v) H_2/N_2 gas flow rate of 20 cm^3 min^{-1}, from RT to 900 °C at 10 °C min^{-1}. The response was measured with a thermal conducting detector.

2.3 Catalytic Activity

The catalytic properties were determined in a flow system through a fixed bed quartz reactor with an inner diameter of 9 mm connected on line with a Perkin Elmer chromatograph. The catalysts were previously reduced in H_2 stream for 1 h at 650 °C and the catalyst mass used was 0.03 g. The reactor was fed with a flow rate of 100 cm^3 min^{-1} (CH_4/CO_2/He = 7/14/79 cm^3 min^{-1}, CH_4/CO_2 ratio of 0.5). The reaction was tested at 650 °C and atmospheric pressure under conditions of chemical control. The stability of the catalysts was determined in isothermal conditions for 20 h, using a feed $CH_4/CO_2 = 0.5$ to inhibit the spontaneous deposition of carbon.

The reactivity and amount of carbon deposited over samples extracted from reactor after 20 h using a ratio $CH_4/CO_2 = 1.2$ were determined by Temperature-Programmed Oxidation (TPO). Experiments were carried out in a Shidmazu TG-50H thermobalance under air stream between 100 and 900 °C and a gas flow rate of 20 °C min^{-1}.

The Raman spectra were collected using the powder samples at room temperature in the back-scattering geometry with an inVia Renishaw spectrometer equipped with an air-cooled CCD detector and a super-Notch filter. The emission line at 488.5 nm from an Ar+ ion laser and at 788.5 nm of a diode laser was focused on the sample under a Leica DLML microscope using 20× or 5× objectives.

The spectral resolution was 2 cm^{-1}. Spectra were calibrated using the 520.5 cm^{-1} line of a silicon wafer.

The use of laser radiation in the visible and red spectral region can allow a more precise determination of the carbon species, because band position and intensity of some compounds are energy dispersive (dependent on energy radiation).

Band position, integrated band area and full band width at half maximum (FWHM) were determined after background subtraction by a curve fitting procedure with Lorentzian functions using variable position.

3 Results and Discussions

3.1 Morphological Properties

Table 1 summarizes morphological properties of non promoted (Rh/Al) and Ce-promoted (Rh/Ce–Al) catalysts, to analyze the effect of ceria addition and calcination temperature, taking ceria-α-alumina support as reference. No significant changes are observed in the textural properties of support by the Ce addition. In the Rh/CeAl catalysts after reaction there is slightly change in the textural properties.

3.2 X-ray Diffraction

The XRD analysis of different samples permits to identify the peaks of α-Al_2O_3 and CeO_2. From the diffractograms in Fig. 1, it is possible to observe the characteristic peaks of Ce for the values of 2θ = 28, 33, 47 and 56°, the rest of the peaks corresponds to α-Al_2O_3. However, no diffraction line referring to Rh species was detected in fresh and reduced samples, which can be attributed to low noble metal loading.

Table 1 Morphological characteristics of the catalysts

Materials	Calcination temperature (°C)[a]	Specific area (m^2/g)	Pore volume (cm^3/g)
Al_2O_3	500	5	0.01
Ce–Al	500	10	0.05
Rh/Al	350	10	0.016
Rh/Al	500	8	0.013
Rh/Ce(3) Al	350	6	0.022
Rh/Ce(5) Al	350	10	0.033
Rh/Ce(5) Al	500	8	0.035
Rh/Al used	350	8	0.010
Rh/Ce(5)Al used	350	11	0.040

[a] Calcination temperature after Rh addition

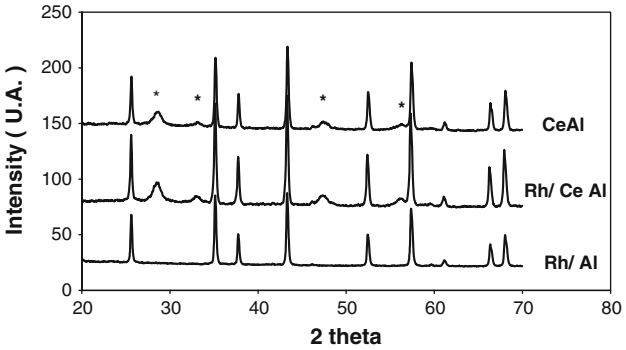

Fig. 1 XRD patterns of modified support CeO_2-α Al_2O_3 and reduced Rh/α-Al_2O_3 and RhNi/CeO_2-α-Al_2O_3 catalysts. (*) Ce peaks

3.3 Temperature Programmed Reduction

The thermograms of the catalysts and CeO_2–Al_2O_3 support are shown in Fig. 2. The TPR profiles of Rh/Al (350) show reduction peaks (Fig. 2a) near 180, 240 and 360 °C and a broad feature between 400 and 600 °C. The low temperature peaks could be assigned to the reduction of isolated RhO_x species. The first one is attributed to the reduction of well dispersed Rh_2O_3 particles and the small one is associated with reduction of crystallites in large Rh_2O_3 particles on the support surface [22]. The sharp peak around 380 °C is assigned to reduction of RhO_x species interacted with Al_2O_3. For the samples doped with ceria (Fig. 2b and c) the sharp peak about 140 °C corresponds to the reduction of free Rh_2O_3 as described above. Differing from Rh/Al sample, the peak assigned to the reduction of large Rh_2O_3 particles disappeared. These results suggest a higher Rh dispersion on the ceria promoted than those non-promoted catalysts. In addition there is a second peak at 360 °C assigned to RhOx–Al_2O_3. At higher temperature the reduction peak of ceria seems to overlap with the peak of RhOx–Al_2O_3. These results suggest a significant interaction between Rh and the support which would help to reduce RhOx–Al_2O_3 species and to the CeO_2 near the Rh [12]. Different authors [24–27] propose that the Rh° dissociates H_2 molecules into H atoms, which subsequently spillover onto the surface CeO_2 and promote its reduction but it does not affect the reduction of bulk ceria. Studies of Bernal et al. [28] employing TPR and mass spectroscopy suggest that the hydrogen interaction with the ceria is strictly a surface process. Different authors [29, 30] report that TPR studies of ceria have shown that ceria reduction takes place in two temperature regions with maxima around 520 and 827 °C, respectively. These two reduction regions are attributed to the surface and bulk reduction, respectively.

TPR analysis of Ce Al support (Fig. 2, corner) prepared in our laboratory presents a region containing three peaks

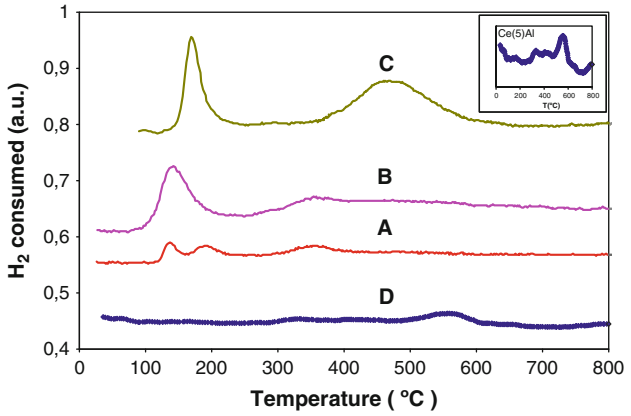

Fig. 2 TPR profiles of (*A*) Rh/α Al_2O_3, (*B*) Rh/Ce-α Al_2O_3 (350), (*C*) Rh/Ce-α Al_2O_3(500), (*D*) Ce-α Al_2O_3 (350). In the corner the Ce-α Al_2O_3 (350) profile is amplified

of low intensity, below 500 °C and a signal of higher intensity at 570 °C with a shoulder at 660 °C. The low temperature peaks are attributed to the presence of surface oxygen ions and the signal at higher temperature can be assigned to the reduction of bulk Ce^{4+} to Ce^{3+} [17, 18].

It is known that the calcination temperature has significant influence in the reducibility of supported Rh species [32]. In Rh/CeAl 500 catalysts, the relative intensity of low temperature TPR peak increases and the maxima shift at higher temperature. The peak-shift detected in the Rh/CeAl (500) suggests a stronger interaction between Rh and CeO_2 which retard the reduction of isolated RhOx. In this sample other peaks are observed at highest temperature, which are assignable to a higher interaction between the Rh and the neighboring species. In many alumina supported metals, the reduction of species at higher temperature has been reported as MAl_2O_4 spinel species (M = Pd, Pt, Ni, Cu, Co). Wang et al. [18] reported the formation of $(RhO_2)_y$ species by diffusion into the sub-layers of the alumina structure at high temperature. The presence of species strongly interacted with the Al_2O_3 would explain the activity loss of Rh catalyst supported on alumina after thermal aging or high temperature calcination in an oxidizing environment [31, 32]. As the reduction peak of Rh seemed to overlap with that of the surface ceria, the amount of H_2 consumed largely exceeded the amount needed for total reduction of Rh_2O_3.

3.4 Catalytic Activity and Selectivity

Catalysts were evaluated in the reaction of dry reforming of methane in chemical control conditions analyzing the performance for 20 h. In order to compare the methane conversions, experiments were performed at the same space time and feed composition. Figure 3 shows the CH_4 conversion as a function of time on stream on Rh/Ce(x)-Al(350) and Rh/Al(350) catalysts, at 650 °C with a CH_4/CO_2 ratio of 0.5. According to thermodynamic data, this ratio inhibits the spontaneous carbon deposition. In these conditions, the Rh/Ce (5) Al(T) presents the highest conversion level and stability in time on stream. The support modification with Ce helps to improve the catalytic activity, so greatly increasing the methane conversion. Table 2 shows the initial activity and stability after 15 h in reaction for the promoted and non-promoted catalysts. The conversion of CH_4 and CO_2 increases with the Ce content increase in promoted system for the same catalyst calcination temperature. The selectivity defined as H_2/CO ratios has the same trend with the increasing CeO_2 content. The H_2/CO ratio for all catalysts is minor than one, in agreement with the literature, as consequence of the occurrence of reverse of water–gas-shift reaction [33]. It has been reported that the dry reforming of methane is a sensitive structure reaction and the rate of methane activation increases with higher dispersion [32]. Therefore the enhanced activity can be related to a significantly higher Rh dispersion on the CeO_2–Al_2O_3 support [34]. In order to check the aforementioned phenomena, the Rh metallic area and dispersion were determined by H_2 chemisorption in promoted and non promoted catalysts. In Table 3, the dispersion and specific activities (TOF) for the Rh/Al and Rh/Ce(5)Al catalysts are shown. Noble metal dispersion of 64 and 81% was determined by H_2 chemisorption for Rh/Al and Rh/Ce(5)Al catalysts, respectively. The presence of ceria seems to reduce Rh agglomeration increasing the interface Rh-support and thus making surface Rh sites more available. Regarding the Rh/Al(350) catalyst, it presents a high fall in initial methane conversion with respect to the ceria promoted catalyst calcined at the same temperature. Probably, the greatest initial deactivation suffered by the Rh/Al_2O_3 catalyst is likely driven by process of surface transformation of dispersed particles into bigger ones during reaction.

Referring to stability of catalysts, evaluated in terms of the activity coefficient (a_{CH4}), the highest is the one for Ce promoted catalysts (Table 2). Catalysts calcined at 500 °C had shown the most favorable stability profile due to the relatively low conversion level at the beginning of the reaction, which is attributed to a higher interaction of Rh with the support, according with TPR results that affected the catalyst performance.

It is known that CeO_2 is a support with a large capacity to store oxygen that facilitates the mobility of active species on the surface by means of hydrogen spillover mechanisms, which could be very favorable for the DRM reaction, as the speed by which the Rh recuperates its metallic state as a fundamental condition for its activity.

From the industrial point of view it may be desirable to operate with CH_4/CO_2 ratios close to unity but in this

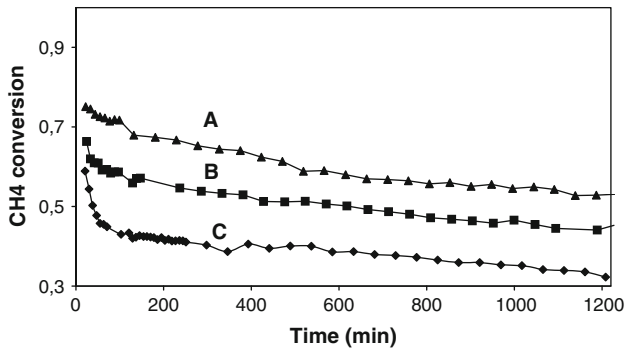

Fig. 3 CH_4 conversion vs. time on stream for non promoted and Ce promoted Rh/α Al_2O_3 catalysts at 650 °C and CH_4/CO_2ratio = 0.5. (*A*) Rh/Ce(5)Al(350), (*B*) Rh/Ce(3)Al(350), (*C*) Rh/Al catalysts

condition the carbon formation is thermodynamically favored. Therefore, catalysts were tested at 650 °C and $CH_4/CO_2 = 1.2$ ratio for 20 h, with the aim of analyzing the activity and stability under these conditions. Figure 4 shows the variation of the activity coefficient (x/xo, CH_4 conversion at time t vs. initial CH_4 conversion), over the different samples as a function of time on stream. Under these reaction conditions the Rh/Ce(x)Al(350) catalysts have shown high stability throughout the time whereas the Rh/Al(350) presents a strong deactivation in less than 5 h in reaction. A total deactivation after 20 h in reaction was found for the non promoted catalyst and the methane conversion falls up around zero. The deactivation may be associated to metal sintering and/or carbon deposition. In this case, the TEM analysis of catalysts after reaction shows the presence of carbon nanotubes. Therefore, the decrease in activity is attributed to the carbon deposition.

3.5 Carbon Deposition Characterization

After 20 h in reaction, the samples were extracted from reactor and the amount of carbon deposited was determined by TPO in a thermobalance on air stream at programmed temperature. In Fig. 5 it is possible to observe that the Rh/Al catalyst shows an important weight loss (29%) from 400 to 700 °C with a maximum around 580 °C assignable to a single type of carbon, suggesting the formation of filamentous carbon species, what could result in a drawback

Table 3 Chemisorption characterization of the catalysts

Catalysts	H_2 adsorption ($\mu mol/g_{\cdot cat}$)	D (%)	A_M (m^2/g_{Rh})	TON (s^{-1})
Rh/Al	32	64	289	47
Rh/Ce(5)Al	40	81	361	79

for their application at large scale. The Rh/Ce–Al catalysts do not exhibit weight loss which indicates that the addition of Ce inhibits the carbon formation. This result can be explained by the chemical properties. One possible reason is the presence of Ce^{4+}/Ce^{+3} redox couple, which makes that the CO_2 is more readily activated to release more surface oxygen, and the rate of carbon elimination is accelerated [18]. The ability of ceria to storage oxygen and its redox properties could contribute to the combustion of deposited carbon on the active sites decreasing the deactivation rate by coke. On the other hand, it is known that metallic catalysts need larger ensembles for carbon formation whisker type [35–38]. Probably, ceria can aid in the stabilization of Rh dispersion and avoids the minimum ensemble necessary for carbon deposition. In Fig. 6, the TEM image of the used Rh/Al catalyst provides clear evidence that the carbon formed during the reaction was in the form of filamentous whiskers. The possibility of smaller amount of graphitic carbon blocking active sites could not be excluded.

In order to characterize the structure of the carbon deposited during the reforming reaction, the Raman spectra of catalysts after reaction were registered. The Raman spectra of graphite present two main bands: (i) The band G appearing in the 1500–1700 cm^{-1} which provides information about the electronic properties of filamentous carbons and is a measurement of the presence of ordered carbon and (ii) the band D in the range 1285–1355 cm^{-1} which is characteristic of single or multiwalled rolled sheets, SWCNT and MWCNT, respectively. The various carbon forms can be distinguished by the position and the line width (FWHM) of the D band [39–41].

In the Raman spectra of Rh/Al sample extracted from reactor, the presence of SWCNT is clearly evidenced in the spectrum in Fig. 7, by the narrow peak at about 148 cm^{-1} and by the position of the D band at about 1300 cm^{-1}. The downshift of the D band (FWHM value 60 cm^{-1}), about

Table 2 Catalytic activity and selectivity at 650 °C and (CH_4/CO_2) = 0.5

Catalysts	Final calcination temperature (°C)	$X_{CH4(1h)}$	$X_{CO2(1h)}$	H_2/CO	a^a_{CH4}
Rh/Al	350	0.46	0.32	0.55	0.54
Rh/Al	500	0.49	0.27	0.78	0.69
Rh/Ce(3%)–Al	350	0.59	0.44	0.61	0.70
Rh/Ce(5%)–Al	350	0.72	0.47	0.70	0.70
Rh/Ce(5%)–Al	500	0.47	0.30	0.67	0.84

[a] Activity coefficient defined as the ratio between the conversion during 15 h and the initial conversion

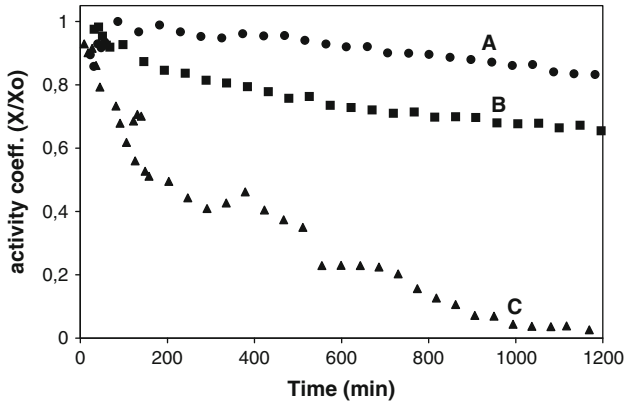

Fig. 4 Stability test of non promoted and Ce promoted Rh/α Al_2O_3 catalysts (650 °C and CH_4/CO_2 ratio =1.2). (*a*) Rh/Ce(5)Al(350), (*b*) Rh/Ce(3)Al(350), (*c*) Rh/Al catalysts

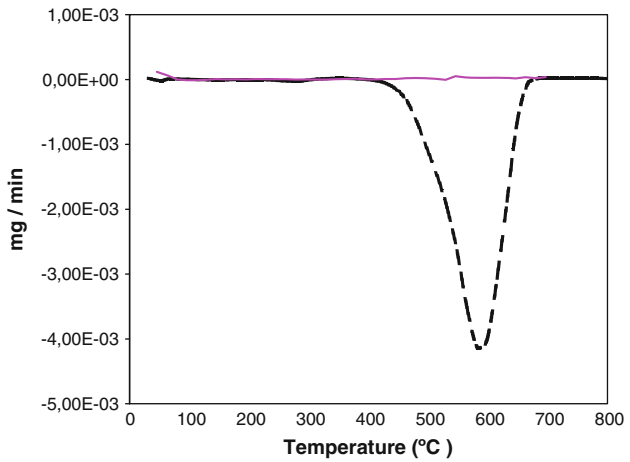

Fig. 5 Derivative of weight variation as function of temperature for Rh/Ce(5%)Al (*solid line*) and Rh/Al (*broken line*) catalysts after 20 h in reaction at 650 °C and a ratio CH_4/CO_2=1.2. Experiments were carried out under air stream between 100 and 900 °C and a gas flow rate of 20 °C min^{-1}

1305 cm^{-1}, and the sharp G band (FWHM value 40 cm^{-1}) at about 1594 cm^{-1} strongly support the presence of SWCNT, although a certain amount of poorly organized carbon species is evident.

In Rh/Ce(5%)Al catalyst, the spectra in Fig. 8 shows a most prominent feature at about 461 cm^{-1}, due to CeO_2. The D (1320 cm^{-1}) and G (1600 cm^{-1}) bands are broad and appear together with other components indicating the presence of various ill-organized carbon species. The carbon region, in the range 1000–2000 cm^{-1}, results in a complex and poorly resolved structure. The D (∼1320 cm^{-1}) and G (∼1600 cm^{-1}) bands are broad and appear together with other components indicating the presence of various ill-organized carbon species. However, in these catalysts, the low intensity of the bands suggests that the carbon amount is negligible.

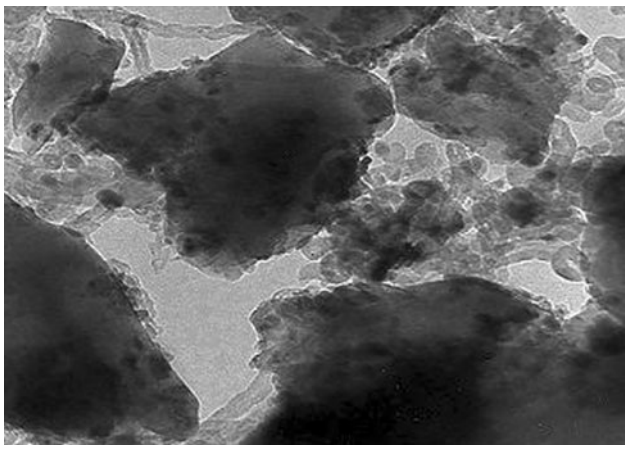

Fig. 6 TEM micrograph of Rh/Ce–Al after 20 h in reaction

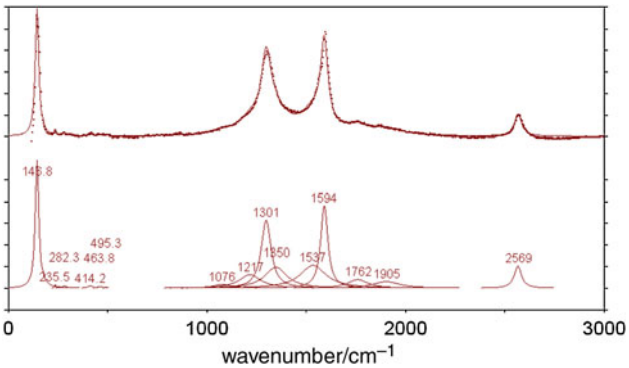

Fig. 7 Curve fit results of Raman spectrum of Rh/Al sample after DRM reaction at 650 °C and CH_4/CO_2=1.2 ratio, examined with the 785.0 nm laser line

The relative size of the bands shows that the formation of ordered carbon species, such as carbon nanotubes and filamentous carbon were formed during reforming reaction over Rh/Al sample, although a certain amount of poorly organized carbon species is evident.

Considering that the whisker-like filamentous carbon is responsible for the destruction of catalyst structure and produce hot spots in the reactor, the development of Rh/CeAl catalysts is important since they inhibit their formation. These catalysts could be an alternative, especially in industrial operations [36–38].

4 Conclusions

Ce promoted Rh/Al catalysts, at low Rh content, show a very important performance for the dry reforming of methane. The Ce promoted catalysts present a higher activity and stability and inhibits the carbon deposition on the catalyst. Results show that the activity in dry reforming of methane depends on the Ce content and the calcination temperature. Catalyst with 5% of ceria loading has shown

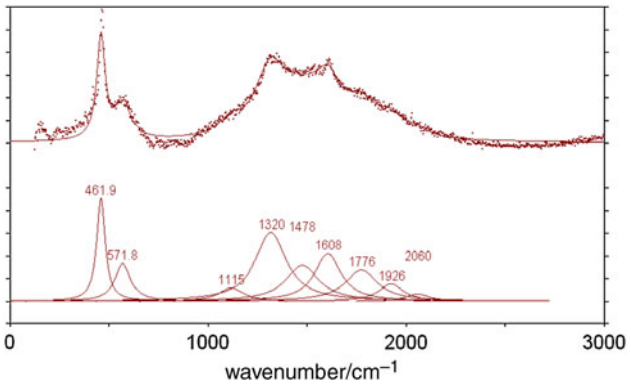

Fig. 8 Curve fit results of Raman spectrum of Rh/CeAl sample after DRM reaction at 650 °C and CH_4/CO_2=1.2 ratio, examined with the 785.0 nm laser line

the best performance according with a high Rh dispersion and metal surface area, evaluated by H_2 chemisorption and TPR analysis.

From this report, it is possible to note that the incorporation of Ce in Rh/Al catalysts could add properties to Rh based catalyst that contribute to improve the catalytic activity for the dry reforming of methane in aspects like thermal stability, carbon formation and metallic dispersion.

Acknowledgments Authors are grateful to CONICET, UNLP, ANPCyT and Università di Roma "La Sapienza", for their financial support of this work.

References

1. Bradford MCJ, Vannice MA (1999) CO_2 reforming of methane. Catal Rev Sci Eng 41:1
2. York APE, Xiao TC, Green MLH, Claridge JB (2007) Methane oxireforming for gas synthesis production. Catal Rev Sci Eng 49:511
3. Souza MMVM, Aranda DAG, Schmal M (2001) Reforming of methane with carbon dioxide over Pt/ZrO_2/Al_2O_3 catalysts. J Catal 204:498
4. Bradford MCJ, Vannice MA (1998) CO_2 reforming of CH_4 over supported Pt catalyst. J Catal 173:157
5. Williams SM, Noronha FB, Fendley G, Resasco DE (2000) CO2 reforming of CH_4 over Pt/ZrO_2 catalyst promoted with La and Ce oxides. J Catal 194:240
6. Silva PP, Silva FA, Souza H, Lobo AG, Mattos LV, Noronha FB, Hori CE (2005) Partial oxidation of methane using Pt/Ce-ZrO_2/Al_2O_3 catalysts—effect of preparation methods. Catal Today 101:31
7. Wang HY, Ruckenstein E (2000) Carbon dioxide reforming of methane to synthesis gas over supported rhodium catalysts: the effect of support. Appl Catal A 204:143
8. Ocsachoque M, Quincoces CE, González MG (2007) Effect of Rh addition on activity and stability over Ni/γ-Al_2O_3 catalysts. Stud Surf Sci Catal 167:397
9. Shulz PG, González MG, Quincoces CE, Gigola C (2005) Methane reforming with carbon dioxide. The behavior of Pd/α-Al_2O_3 and Pd-CeOx/α-Al_2O_3 catalysts. Ind Eng Chem Res 44:9020
10. Ferreira-Aparicio P, Fernandez-Garcia M, Guerrero-Ruiz A, Rodriguez-Ramos I (2000) Evaluation of the role of the metal support interfacial centers in the dry reforming of methane on alumina supported rhodio catalysts. J Catal 190(2):296
11. Nagai M, Nakahira K, Ozawa Y, Namiki Y, Suzuki Y (2007) CO_2 reforming of methane on Rh/Al_2O_3 catalyst. Chem Eng Sci 62:4998
12. Portugal UL, Santos A, Damyanova S, Marques CMP, Bueno JMC (2002) CO_2 reforming of CH_4 over Rh-containing catalysts. J Mol Catal A 184(1–2):311
13. Quincoces CE, Dicundo S, Alvarez AM, González MG (2001) Effect of addition of CaO on Ni/Al_2O_3 catalysts over CO_2 reforming of methane. Mater Lett 50:21
14. Pompeo F, Nichio NN, González MG, Montes M (2005) Characterization of Ni/SiO_2 and Ni/Li-SiO_2 catalysts for methane dry reforming. Catal Today 107–108:856
15. Tomishige K, Chen YG, Fujimoto K (1999) Studies in carbon deposition on CO_2 reforming of methane over nickel-magnesia solid solution catalyst. J Catal 181:91
16. Nandini A, Pant KK, Dhinga SC (2006) Kinetic study of the catalytic carbon dioxide reforming of methane to synthesis gas over Ni-K/CeO_2-Al_2O_3 catalyst. Appl Catal A Gen 308:119
17. Salazar-Villalpando MD, Reyes B (2009) H_2 production over Ni/Ceria supported catalysts by OPM. Int J Hydrog Energy 34:9723
18. Wang R, Xu H, Liu X, Ge Q, Li W (2006) Role of redox couples of $Rh^o/Rh^{\delta+}$ and Ce^{4+}/Ce^{3+} in CH_4/CO_2 reforming over Rh-CeO_2/Al_2O_3 catalyst. Appl Catal A Gen 305:204
19. Herrmann JM, Ramaroson E, Tempere JF, Barteau MA (1989) Semiconductivity studies of ceria supported nickel related to its methanation catalytic activity. Appl Catal 53:117
20. Barrault J, Chafik A, Gallezot P (1999) Conversion of carbon oxides on carbon supported, nickel-rare earth catalysts. Appl Catal 67:257
21. Trovarelli A, de Leitenburg C, Boaro M, Dolcetti G (1999) The utilization of ceria in industrial catalysis. Catal Today 50:353
22. Kugai J, Subramani V, Song C, Engelhard MH, Chin Y-H (2006) Effects of nanocrystalline CeO_2 supports on the properties and performance of Ni-Rh bimetallic catalyst for Oxidative reforming of ethanol. J Catal 238:430
23. Eriksson S, Rojas S, Boutonnet M, Fierro JLG (2007) Effect of Ce doping on Rh/ZrO_2 catalysts for partial oxidation of methane. Appl Catal A 326:8
24. Ramirez-Cabrera E, Atkinson A, Chadwick D (2002) Reactivity of ceria Gd and Nb-doped ceria to methane. Appl Catal B 36:193
25. Ramirez-Cabrera E, Laosiripojana N, Atkinson A, Chadwick D (2003) Methane conversion over Nb-doped ceria. Catal Today 78:433
26. Strohm JJ, Zheng J, Song C (2006) Low-temperature steam reforming of jet fuel in the absence and presence of sulfur over Rh and Rh-Ni catalysts for fuel cells. J Catal 238:309
27. Ranga Rao G (1999) Influence of metal particles on the reduction properties of ceria based materials studied by TPR. Bull Mater Sci 22(2):89
28. Bernal S, Calving JJ, Cifredo GA, Rodríguez-Izquierdo JM, Perrichon V, Laachir A (1992) Reversibility of hydrogen chemisorption on a ceria-supported rhodium catalyst. J Catal 137:1
29. Ranga Rao G, Mishra BG (2003) Structural, redox and catalytic chemistry of ceria based materials. Bull Catal Soc India 2:122
30. Wang JA, Lopez T, Bokhimi X, Novaro O (2005) Phase composition, reducibility and catalytic activity of Rh/zirconia and Rh/zirconia-ceria catalysts. J Mol Catal A 239:249
31. Hwang C-P, Yeh C-T, Zhu Q (1999) Rhodium oxide species formed on progressive oxidation of rhodium clusters dispersed on alumina. Catal Today 51:93
32. Weng W-Z, Pei X-Q, Li J-M, Luo C-R, Liu Y, Lin H-Q, Huang C-J, Wan H-L (2006) Effects of calcination temperatures on the

catalytic performance of Rh/Al_2O_3 for methane partial oxidation to synthesis gas. Catal Today 117:53
33. Pawelec B, Damyanova S, Arishtirova K, Garcia Fierro JL, Petrov L (2007) Structural and surface features of PtNi catalysts for reforming of methane with CO_2. Appl Catal A 323:188
34. Wang H, Zhu H, Qin Z, Liang F, Wang G, Wanga J (2009) Deactivation of Au/CeO_2-Co_3O_4 catalyst during CO preferential oxidation in H_2-rich stream. J Catal 264:154
35. González MG, Ponzi EN, Ferretti OA, Quincoces CE, Marecot P, Barbier J (2000) Studies on H_2S adsorption and carbon deposition over Mo-Ni/Al_2O_3 catalysts. Adv Sci Technol 18:541
36. Trimm (1977) The formation and removal of coke from Ni catalysts. Catal Rev Sci Eng 16:155
37. Bartholomew CH (1982) Carbon deposition in steam reforming and methanation. Catal Rev Sci Eng 24:67
38. Rostrup-Nielsen JR (1984) In: Anderson JR, Boudart M (eds) Catalysis Science and Technology. Springer, Berlin
39. Ubbonaite S, Halldahl L, Svensson G (2008) Raman spectroscopy studies of carbides derived carbons. Carbon 46:1942
40. Ferrari A, Robertson J (2000) Interpretation of Raman spectra of disordered and amorphous carbon. Phys Rev B 61:14095
41. Arepalli S, Nikolaev P, Gorelik O, Hadjiev V, Holmes W, Files B, Yowell L (2004) Protocol for the characterization of single wall carbon nanotube material quality. Carbon 42:1783